Supporting Information

Highly efficient multi-sites synergistic catalysis of a polyoxovanadate-based metal–organic framework for benzylic C-H bonds oxidation

Tian-Yi Dang,[a†] Run-Han Li,[a†] Hong-Rui Tian,[b] Wei Guan,[a] Ying Lu*[a] and Shu-Xia Liu*[a]

[a]*Key Laboratory of Polyoxometalate and Reticular Material Chemistry of the Ministry of Education, College of Chemistry, Northeast Normal University, Changchun, Jilin 130024, P. R. China.*

[b]*Department of Chemistry and Shenzhen Grubbs Institute, Southern University of Science and Technology, Shenzhen, Guangdong 518055, P. R. China*

E-mail: luy968@nenu.edu.cn; liusx@nenu.edu.cn

Table of Contents

1. Crystallographic Data and Structure Refinements

Table S1. Crystallographic data and structure refinement of **1**

Name	**1**
Empirical formula	$C_{28}H_{28}Cu_3N_8O_{12}V_4$
Formula weight	1062.96
Temperature (K)	297.52
Wave length (Å)	0.71073
Crystal system	monoclinic
Space group	$P2_1/c$
a (Å)	16.059(3)
b (Å)	14.643(2)
c (Å)	7.9460(12)
α (deg)	90
β (deg)	108.842(3)
γ (deg)	90
Volume ($Å^3$)	1768.4(5)
Z, Dcalc (Mg/m^3)	2, 1.996
Absorption coefficient (mm^{-1})	2.853
F (000)	1054.0
Crystal size (mm^3)	0.21 × 0.2 × 0.15
θ range (deg)	2.782 to 25.384
index range (deg)	$-19 \le h \le 19$, $-17 \le k \le 17$, $-9 \le l \le 9$
Reflections collected / unique	28158 / 3241 [R_{int} = 0.2036]
Data / restraints / parameters	3241 / 0 / 250
Goodness-of-fit on F^2	1.008
R1, wR_2 ($I > 2\sigma(I)$)	0.0443, 0.0842
R1, wR_2 (all data)	0.1188, 0.1108
Largest diff. peak and hole (e $Å^{-3}$)	0.55, -0.74

$R_1 = \sum||F_o|-|F_c||/\sum|F_o| \cdot wR_2 = [\sum[w(F_o^2-F_c^2)^2]/\sum[w(F_o^2)^2]]^{1/2}$

Table S2. Selected bond lengths [Å] and angles [deg] for **1**

1			
Cu(1)-O(1)	1.888(4)	Cu(1)-O(1)[1]	1.888(4)
Cu(1)-N(4)[2]	1.999(5)	Cu(1)-N(4)[3]	1.999(5)
Cu(2)-O(6)	1.839(4)	Cu(2)-O(2)[4]	2.417(5)
Cu(2)-O(5)	2.465(5)	Cu(2)-N(1)	1.880(5)
V(1)-O(2)	1.598(5)	V(1)-O(1)	1.668(4)
V(1)-O(3)	1.759(4)	V(1)-O(4)	1.780(4)
V(2)-O(4)	1.790(4)	V(2)-O(5)	1.619(4)
V(2)-O(3)[5]	1.806(4)	V(2)-O(6)	1.651(4)
O(1)-Cu(1)-O(1)[1]	180.0	O(1)-Cu(1)-N(4)[2]	90.28(18)
O(1)-Cu(1)-N(4)[3]	89.72(18)	O(1)[1]-Cu(1)-N(4)[3]	90.28(18)
O(1)[1]-Cu(1)-N(4)[2]	89.72(18)	N(4)[2]-Cu(1)-N(4)[3]	180.0
O(6)-Cu(2)-O(2)[4]	90.00(19)	O(6)-Cu(2)-N(1)	163.9(2)
N(1)-Cu(2)-O(2)[4]	100.9(2)	O(2)-V(1)-O(1)	111.4(3)
O(2)-V(1)-O(3)	110.0(2)	O(2)-V(1)-O(4)	107.8(2)
O(1)-V(1)-O(3)	109.4(2)	O(1)-V(1)-O(4)	107.4(2)
O(3)-V(1)-O(4)	110.77(19)	O(6)-V(2)-O(3)[5]	110.0(2)
O(6)-V(2)-O(4)	107.5(2)	O(5)-V(2)-O(6)	110.6(2)
O(5)-V(2)-O(3)[5]	108.9(2)	O(5)-V(2)-O(4)	111.0(2)
O(4)-V(2)-O(3)[5]	108.84(19)		

[1] -X,1-Y,-1-Z; [2] 1-X,-1/2+Y,3/2-Z; [3] -1+X,3/2-Y,-5/2+Z; [4] +X,+Y,1+Z; [5] +X,3/2-Y,1/2+Z.

2. The asymmetric unit of 1

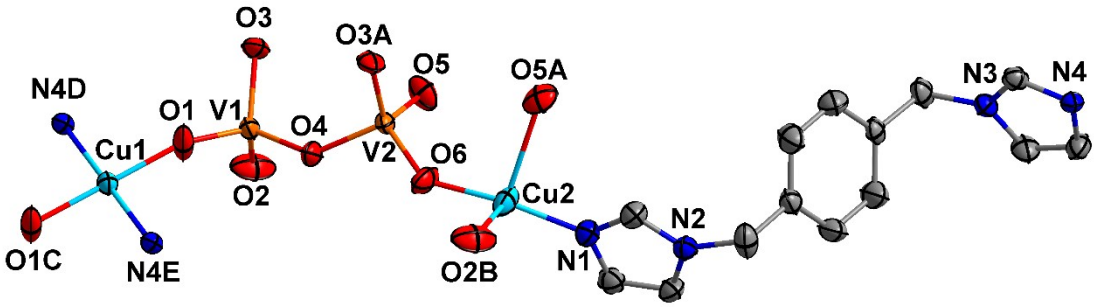

Figure S1. The asymmetric unit of **1**. Asymmetric codes: A, x, 3/2-y, 1/2+z; B, x, y, 1+z; C, -x, 1-y, -1-z; D, -1+x, 3/2-y, -5/2+z; E, 1-x, -1/2+y, 3/2-z.

3. PXRD patterns of 1

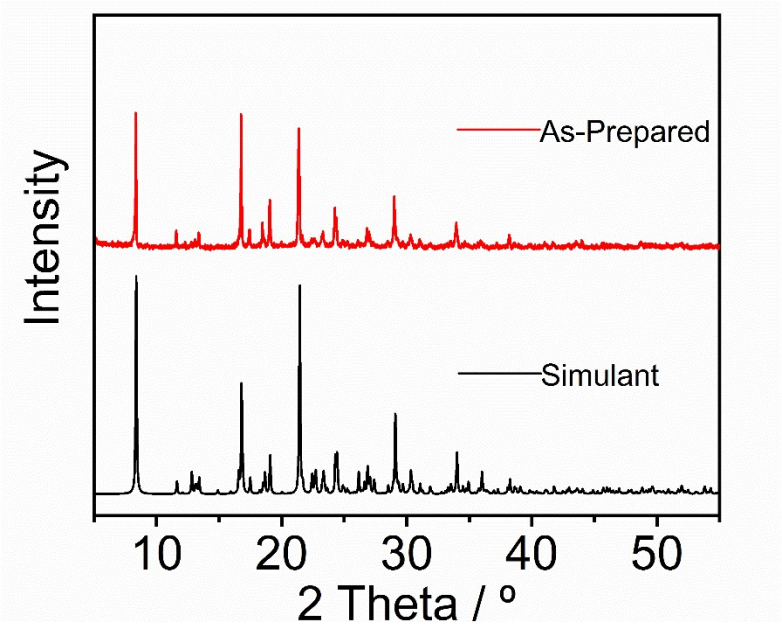

Figure S2. The PXRD patterns of **1**.

4. FTIR Spectrum of 1

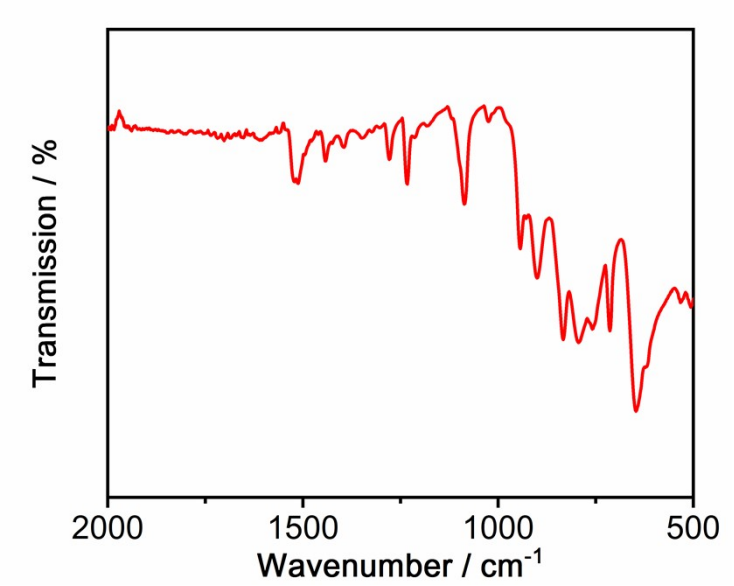

Figure S3. The FTIR spectrum of **1**.

5. XPS Spectra of V and Cu in 1

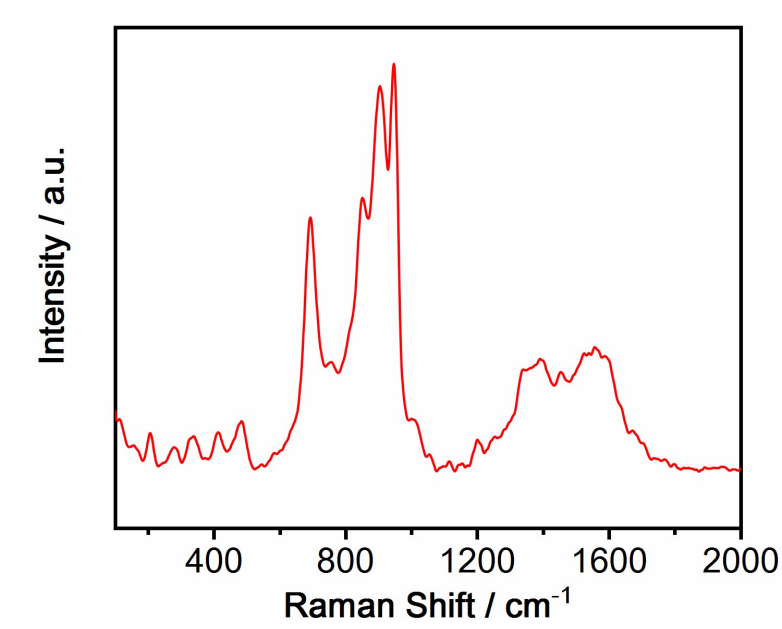

Figure S4. The Raman spectrum of **1**.

6. XPS Spectra of V and Cu in 1

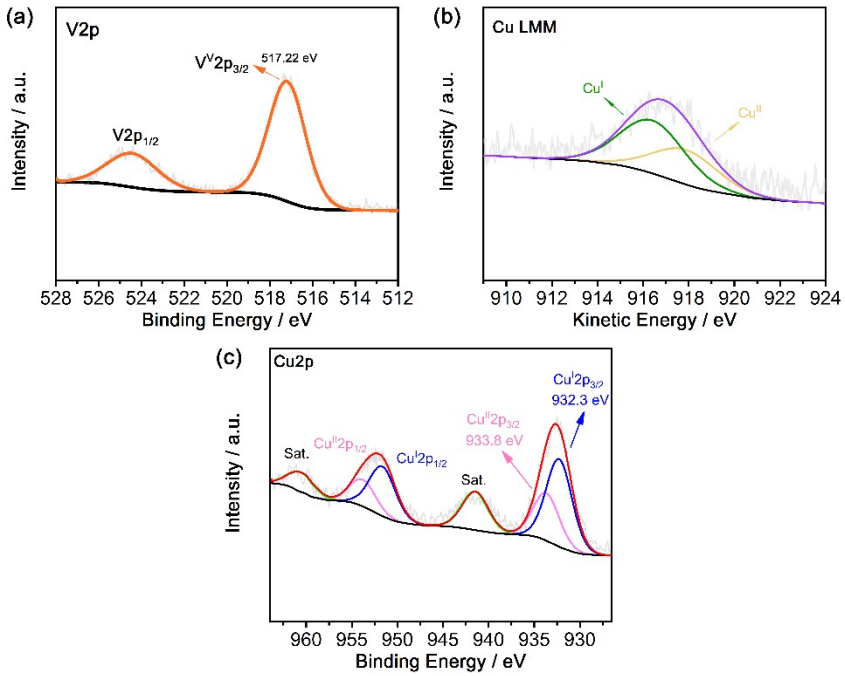

Figure S5. XPS spectra of V (a), Auger spectra of Cu (b) and XPS spectra of Cu (c) in **1**.

7. BVS for the copper ions and vanadium ions in 1

Table S3. BVS results for the copper ions and vanadium ions in **1**

Metal site	BVS cacl.	Assigned O.S.
Cu1	1.282	1
Cu2	1.684	2
V1	5.18	5
V2	5.367	5

8. TGA curve of 1

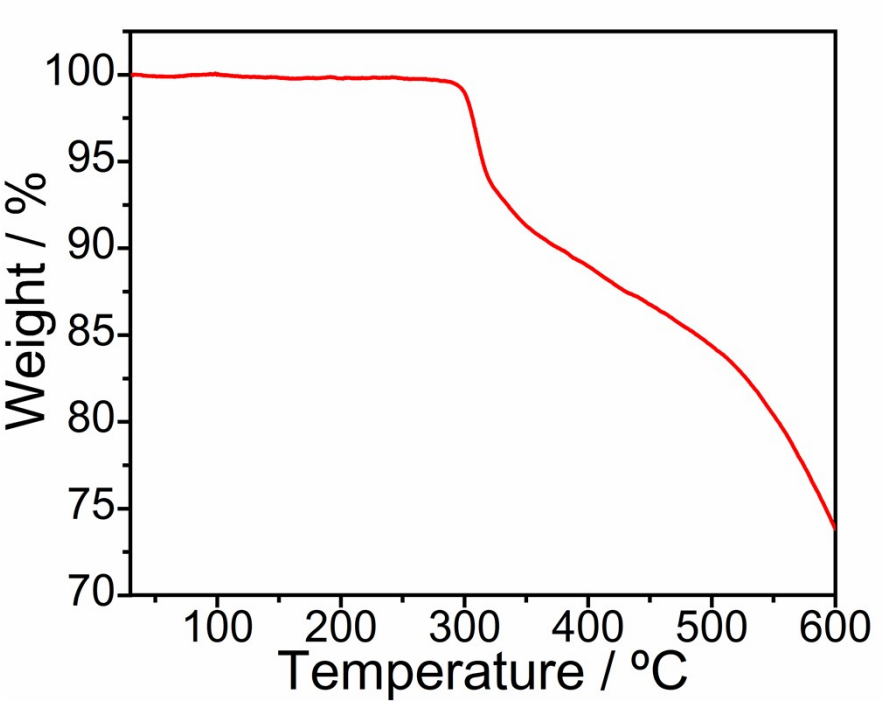

Figure S6. The TGA curve of **1**.

9. PXRD patterns of 1 after immersing in various solvents

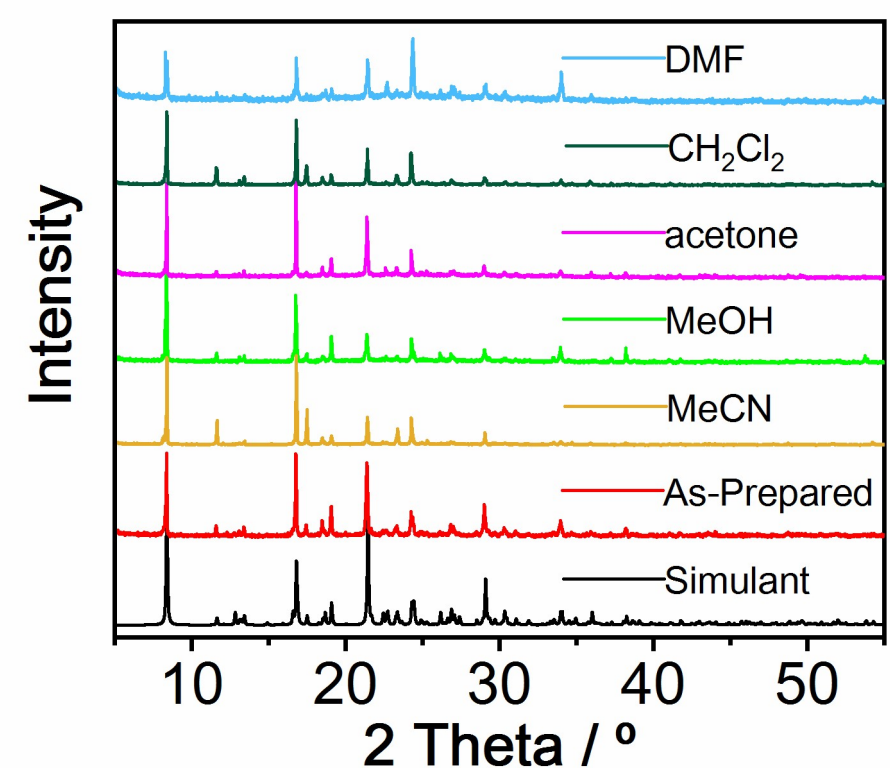

Figure S7. The PXRD patterns of **1** after immersing in various solvents for 7 days.

10. BET analysis of 1

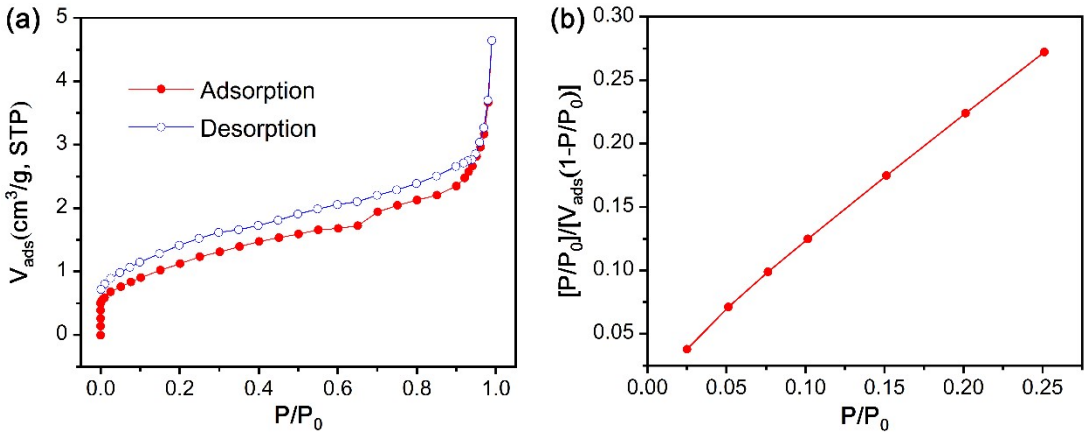

Figure S8. (a) BET analysis of **1**. (b)The N_2 absorption/ desorption isotherms were measured at 77K (P_0 = 101 kPa).

11. Radical trapping experiments

Table S4 Effect of radical trap on the oxidation of indane catalyzed by **1**[a]

Entry	Radical trap	mmol	Yield (%)
1	-	-	96
2	Ph_2NH	0.25	N.D.
3	TEMPO	0.25	52
4	TEMPO	0.50	8

[a]Reaction conditations: indane (0.25 mmol), ^{t}BuOOH (0.75 mmol), **1** (0.0125 mmol, 5% mol), internal standard naphthalene (0.25 mmol), MeCN (2.0 mL), 65 °C,24h.

12. Frontier molecular orbital diagrams of 1

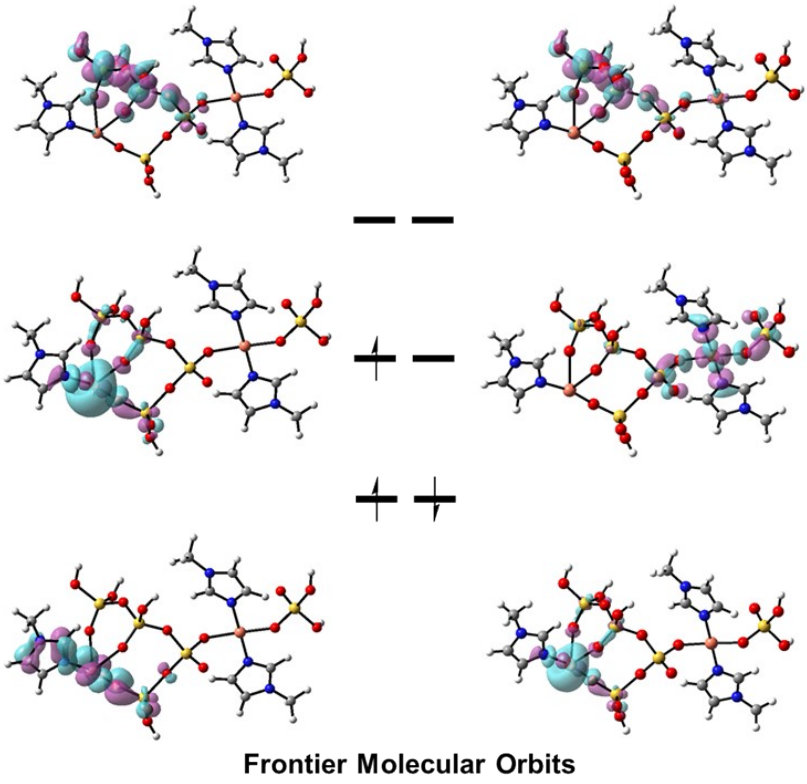

Figure S9 Frontier molecular orbital diagrams of catalyst **1**.

13. Adsorption of ^{t}BuOOH on active sites in 1

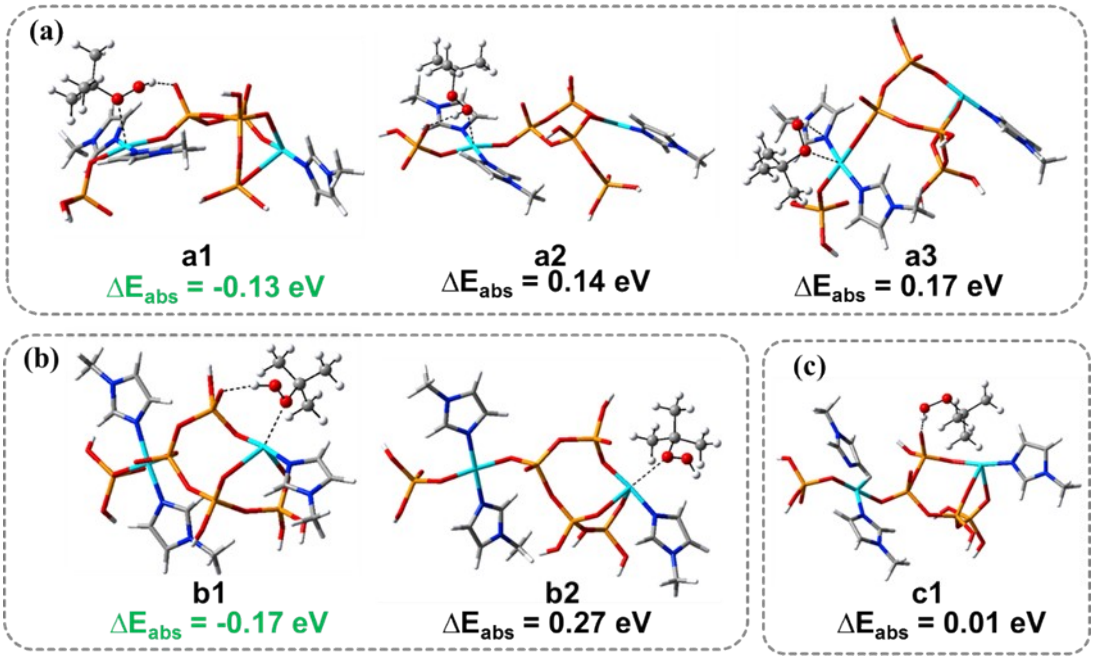

Figure S10 The adsorption of ^{t}BuOOH on Cu^{II}, Cu^{I} and $\{V_4\}$ activated sites of catalyst **1** and the corresponding adsorption energy (eV).

14. Recycling tests of the 1

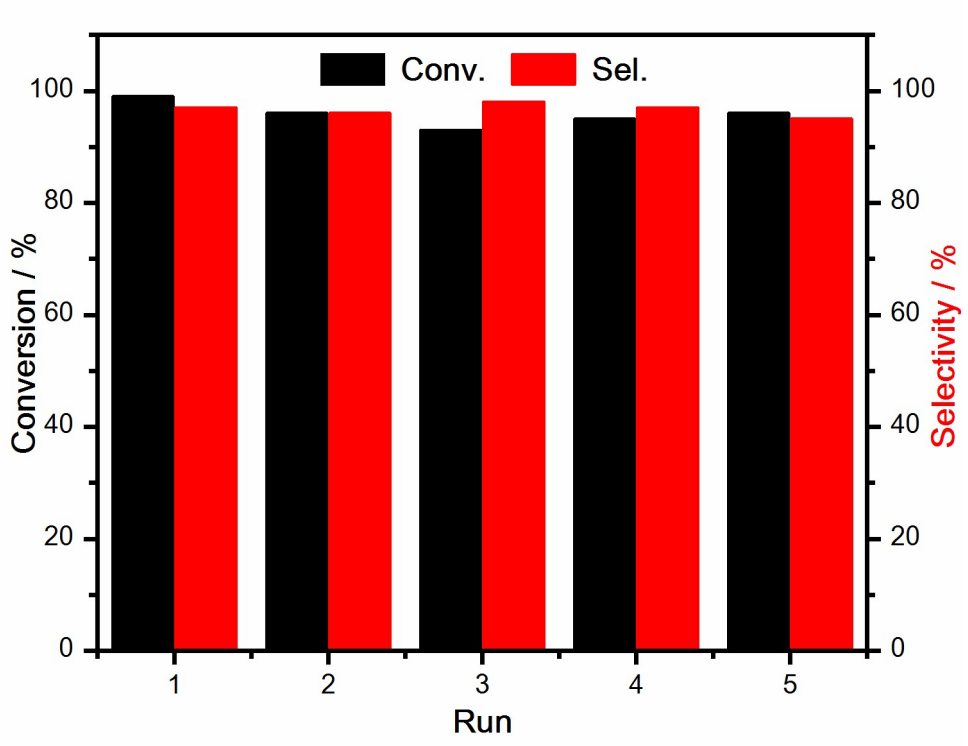

Figure S11. Recycling tests for benzylic compound oxidation using the **1**. Reaction conditations: indane (0.25 mmol), ^{t}BuOOH (0.75 mmol), **1** (0.0125 mmol), naphthalene (0.25 mmol), MeCN (2.0 mL), 65 °C, 24h.

15. SEM images of 1

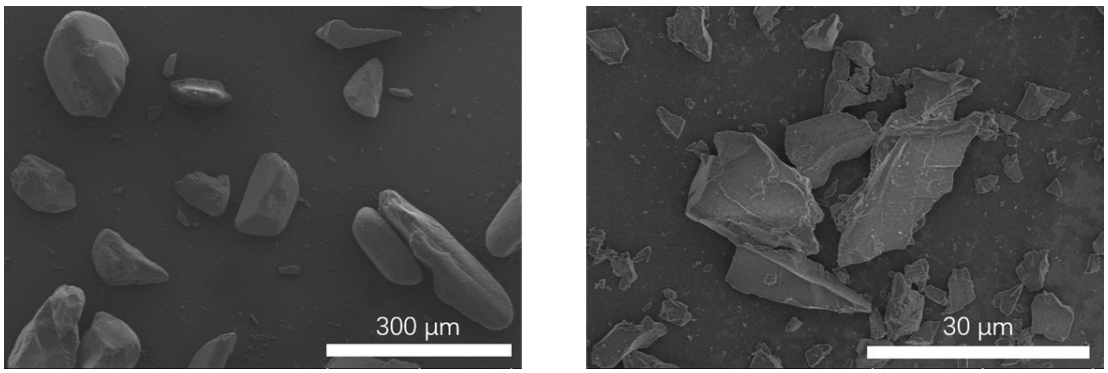

Figure S12. (a) SEM images of the grinded **1**; (b) SEM images of the grinded **1** after benzylic compound oxidation.

16. Comparison of 1 and partially reported catalysts

Table S5 Comparison of **1** and partially reported catalysts

Entry	Catalyst	T (°C)	Yield (%)		Ref.
				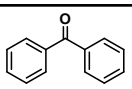	
1	$[Pd(NH_3)_4]_3[V_{10}O_{28}]\cdot 8H_2O$	90	14.7	22.2	1
2	$[Pd(dpa)(acac)]_2[V_6O_{13}(OMe)_6]$	65	73.2	95.8	2
3	$[Cu^I_4L_4]\cdot 4NO_3$	60	16.8	25.2	3
4	$[Na(H_2O)_5](NH_4)_7[P_2W_{15}O_{56}Co_3(H_2O)_3(OH)_3Re(CO)_3]\cdot 13H_2O$	90	87.5	96.8	4
5	$Cu^I_{12}Cl_2(trz)_8[HPW_{12}O_{40}]$	75	97	95	5
6	$[Cu^I_6(trz)_6\{PW_{12}O_{40}\}_2]$	75	90.6	95.2	6
7	$\{[Cd(DMF)_2Mn^{III}(DMF)_2TPyP](PW_{12}O_{40})\}\cdot 2DMF\cdot 5H_2O$	80	92.7	37	7
8	$[Cu_2(C_{33}H_{17}NO_8)(H_2O)]\cdot 3DMF$	65	30	40	8
9	$[Mn_5Cl_2(MnCl\text{-}OCPP)(DMF)_4(H_2O)_4]\cdot 2DMF\cdot 8CH_3COOH\cdot 14H_2O$	65	99	18	9
10	$[Cu^{II}(en)_2]_4\{Na(H_2O)(\mu\text{-}OH)[B(OH)_2]\}_2[(V^VO)_2(V^{IV}O)_{10}O_6(B_{18}O_{36}(OH)_6)]\}\cdot 7H_2O$	65	78.9	-	10
11	Ni-MOF-74/[bmim]Br	60	88	95	11
12	**1**	65	98	96	This work

17. ^{1}H-NMR Spectra of the ketones

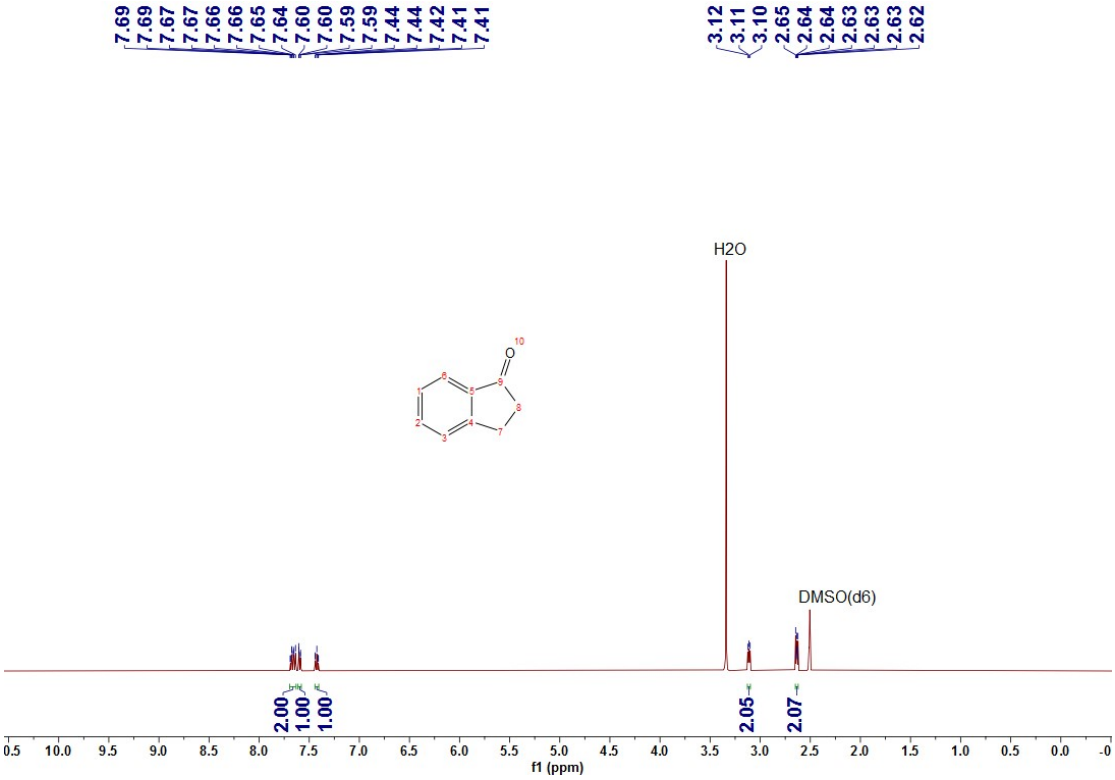

^{1}H-NMR Spectra of 1-indanone.

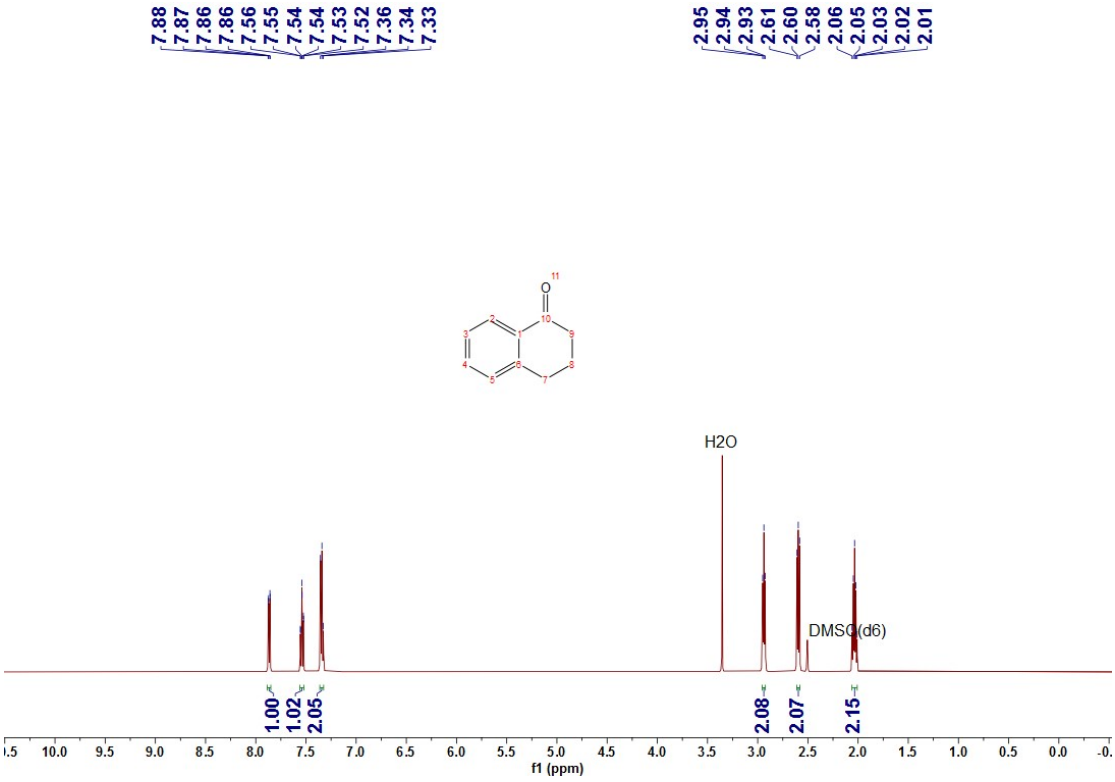

^{1}H-NMR Spectra of α-tetralone.

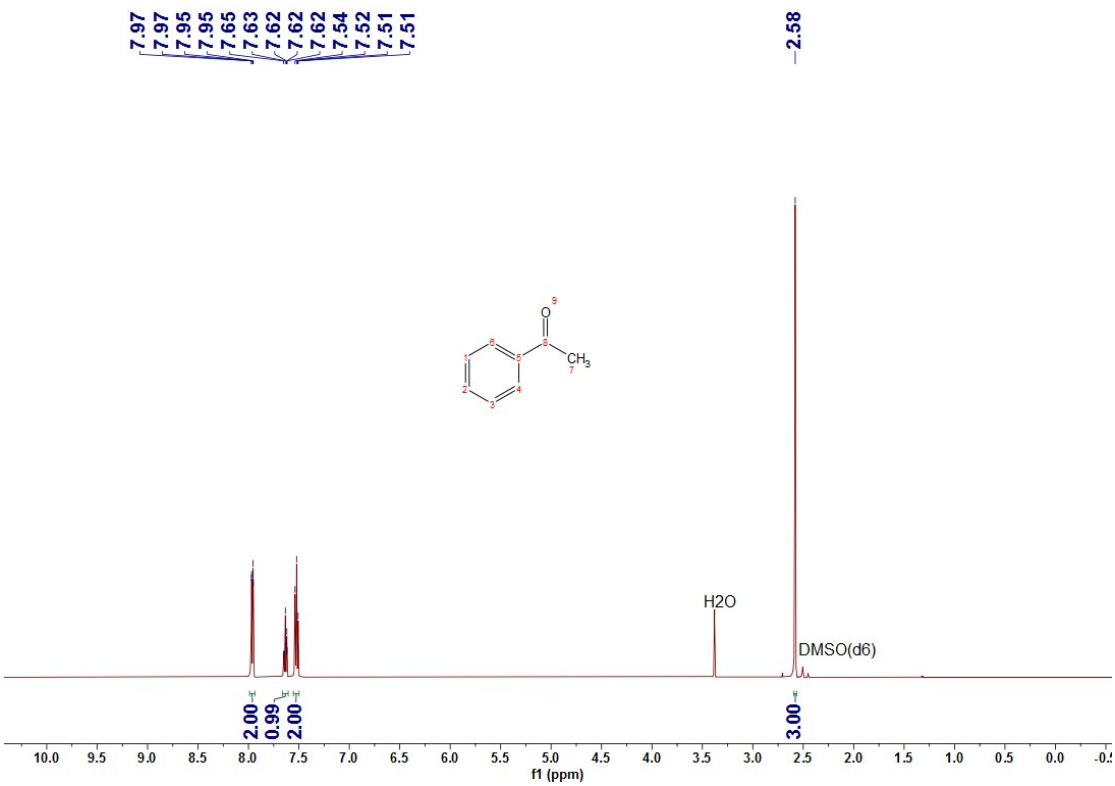

^{1}H-NMR Spectra of acetophenone.

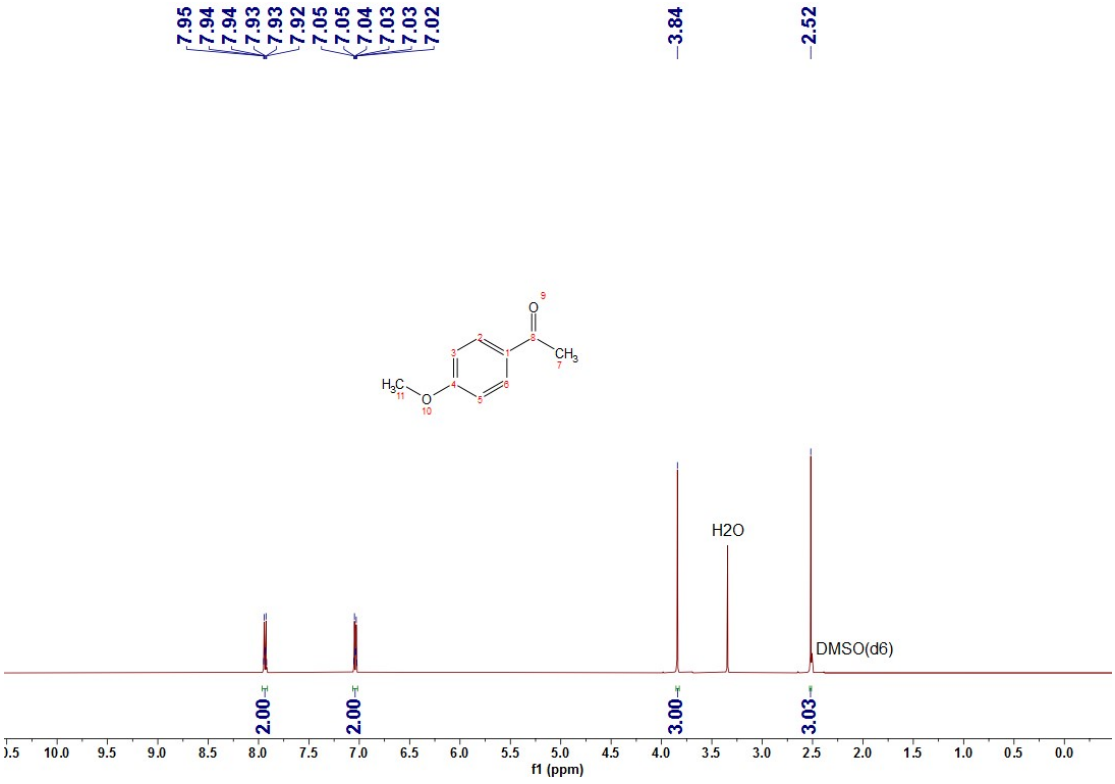

^{1}H-NMR Spectra of 4-methoxyacetophenone.

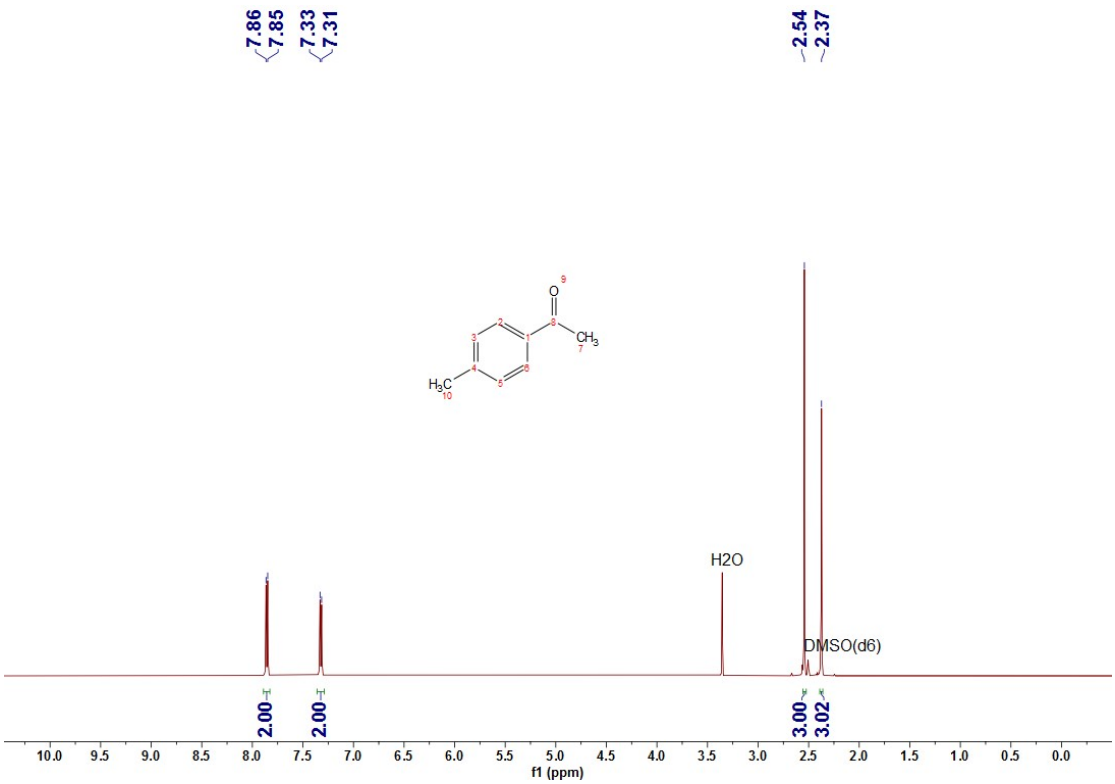

[1]H-NMR Spectra of 4’-methylacetophenone.

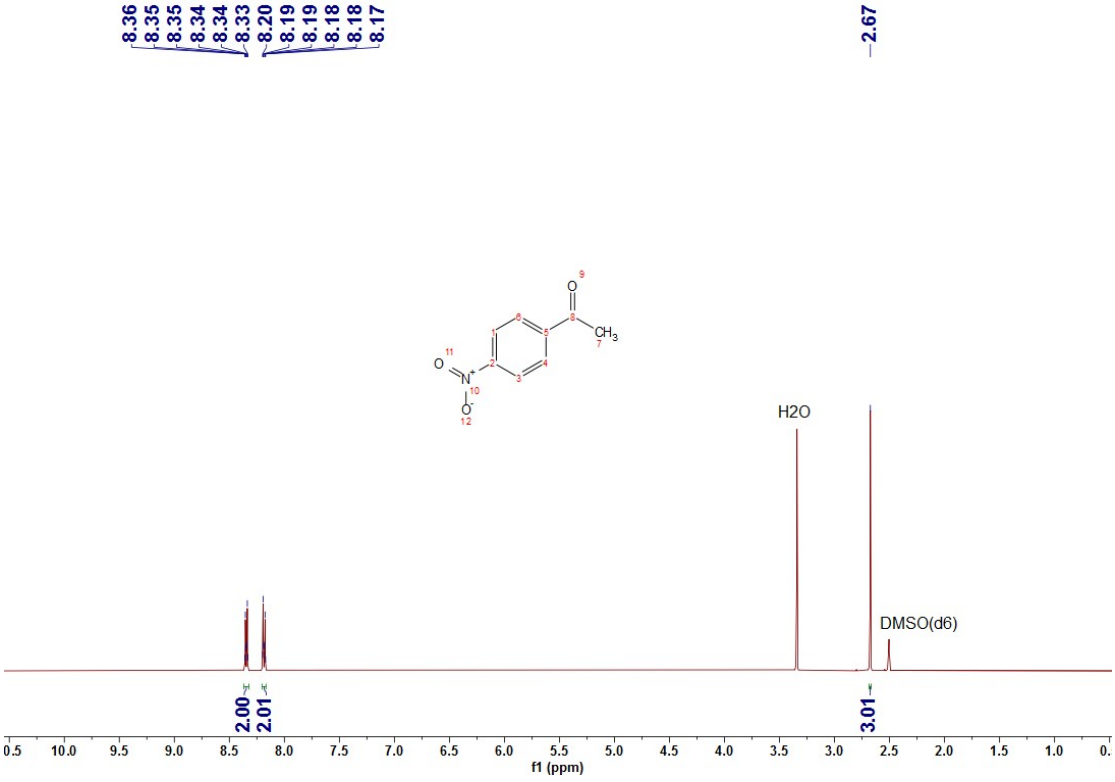

[1]H-NMR Spectra of 4’-nitroacetophenone.

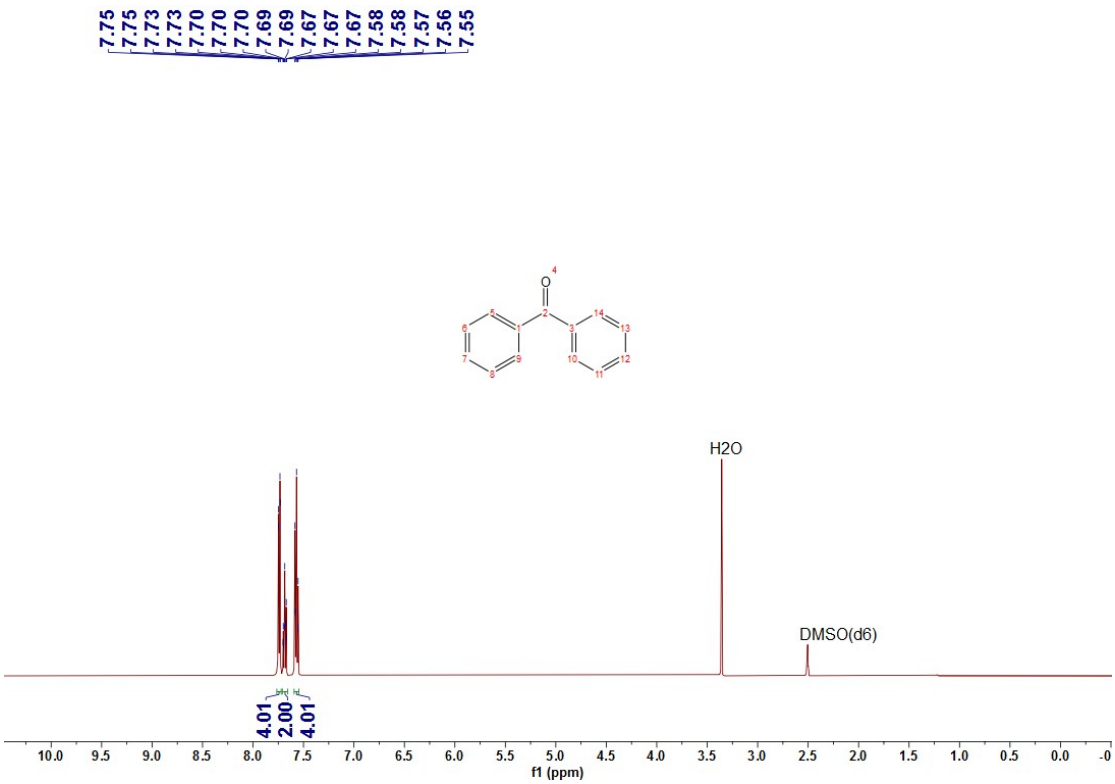

^{1}H-NMR Spectra of benzophenone.

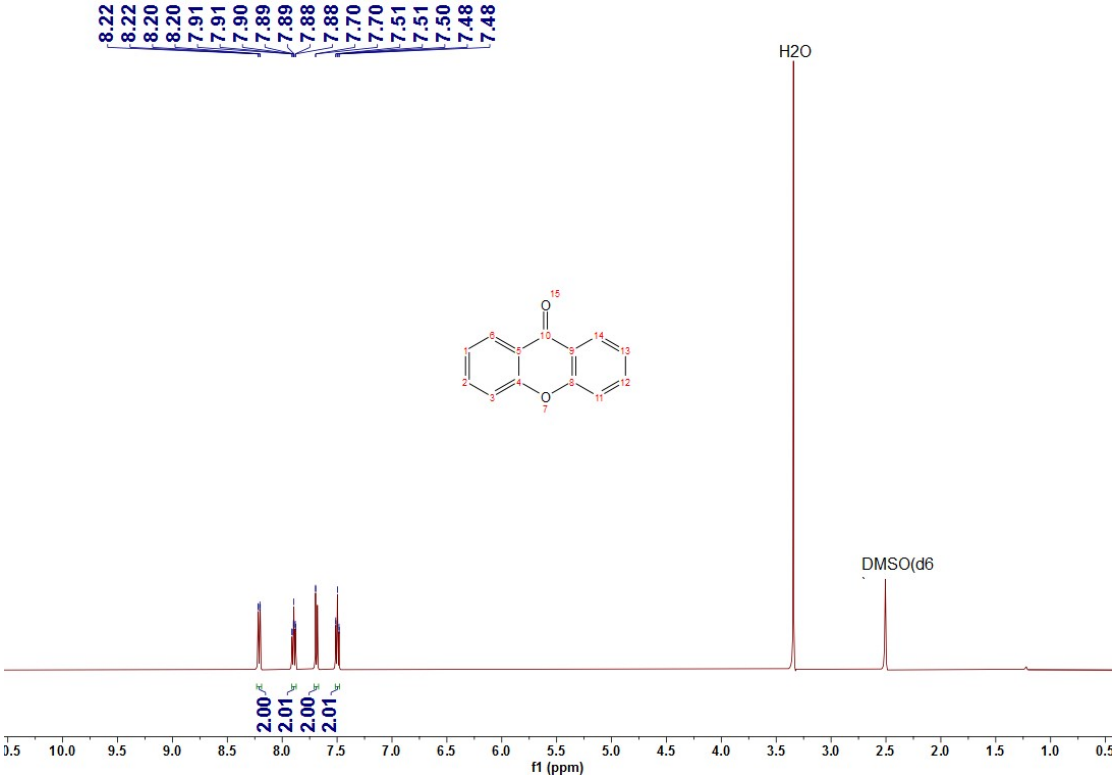

^{1}H-NMR Spectra of xanthone.

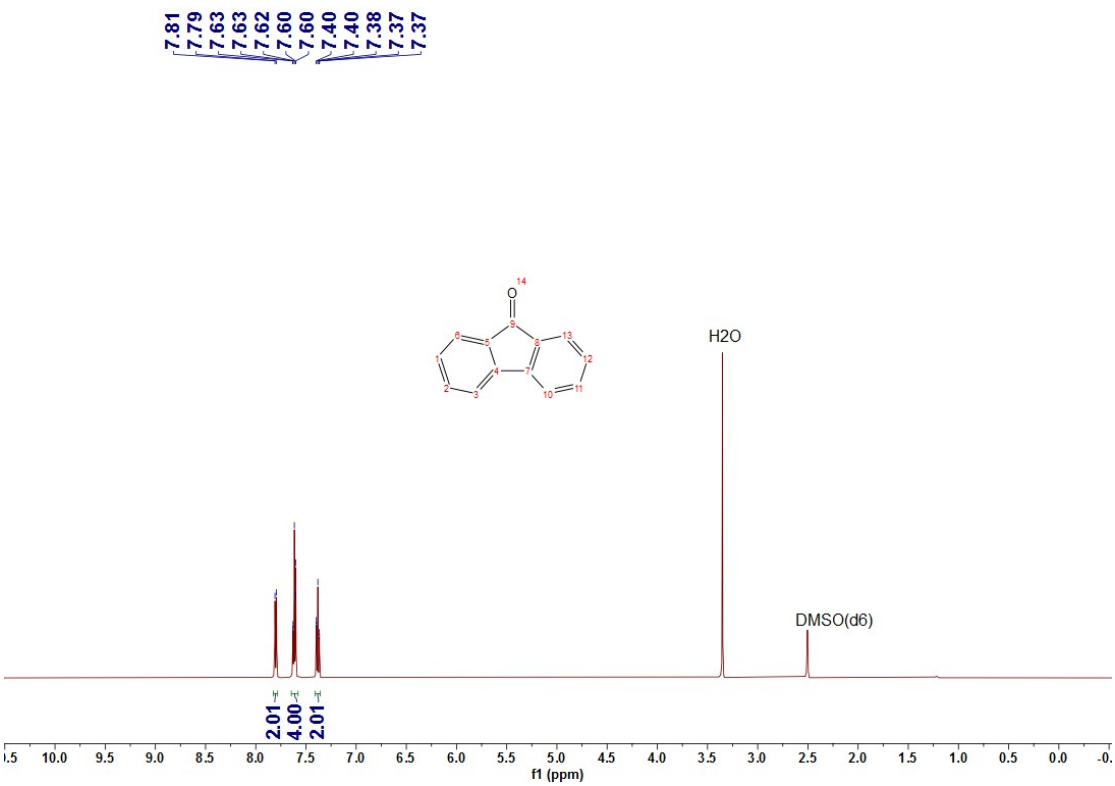

^{1}H-NMR Spectra of 9-fluorenone.

18. References

1. X. Huang, J. Li, G. Shen, N. Xin, Z. Lin, Y. Chi, J. Dou, D. Li and C. Hu, *Dalton Trans.*, 2018, **47**, 726-733.
2. J.-K. Li, X.-Q. Huang, S. Yang, H.-W. Ma, Y.-N. Chi and C.-W. Hu, *Inorg. Chem.*, 2015, **54**, 1454-1461.
3. Q.-T. He, X.-P. Li, L.-F. Chen, L. Zhang, W. Wang and C.-Y. Su, *ACS Catal.*, 2013, **3**, 1-9.
4. X. Ma, P. Wang, Z. Liu, C. Xin, S. Wang, J. Jia, P. Ma, J. Niu and J. Wang, *Inorg. Chem.*, 2020, **59**, 8690-8698.
5. B. Xu, Q. Xu, Q. Wang, Z. Liu, R. Zhao, D. Li, P. Ma, J. Wang and J. Niu, *Inorg. Chem.*, 2021, **60**, 4792-4799.
6. D. Li, X. Ma, Q. Wang, P. Ma, J. Niu and J. Wang, *Inorg. Chem.*, 2019, **58**, 15832-15840.

7. C. Zou, Z. Zhang, X. Xu, Q. Gong, J. Li and C.-D. Wu, *J. Am. Chem. Soc.*, 2012, **134**, 87-90.
8. L. Kimberley, A. M. Sheveleva, J. Li, J. H. Carter, X. Kang, G. L. Smith, X. Han, S. J. Day, C. C. Tang, F. Tuna, E. J. L. McInnes, S. Yang and M. Schröder, *Angew. Chem. Int. Ed.*, 2021, **60**, 15243-15247.
9. X.-L. Yang, M.-H. Xie, C. Zou, Y. He, B. Chen, M. O'Keeffe and C.-D. Wu, *J. Am. Chem. Soc.*, 2012, **134**, 10638-10645.
10. Y. Feng, C. Ding, H. Fan, Z. Zhong, D. Qiu and H. Shi, *Dalton Trans.*, 2015, **44**, 18731-18736.
11. C. Guo, Y. Zhang, Y. Zhang and J. Wang, *Chem. Commun.*, 2018, **54**, 3701-3704.